Constraints on the Fe-S melt connectivity in mantle silicates from electrical impedance measurements

N. Bagdassarov, G.J. Golabek, G. Solferino, M.W. Schmidt

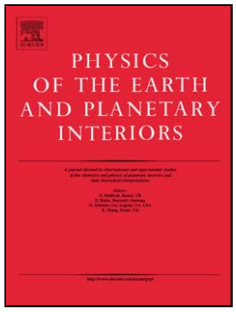

Title: Constraints on the Fe-S melt connectivity in mantle silicates from electrical impedance measurements

Authors: N. Bagdassarov, G.J. Golabek, G. Solferino, M.W. Schmidt

PII: S0031-9201(09)00175-7
DOI: doi:10.1016/j.pepi.2009.08.003
Reference: PEPI 5196

To appear in: *Physics of the Earth and Planetary Interiors*

Received date: 12-12-2008
Revised date: 5-8-2009
Accepted date: 19-8-2009

Please cite this article as: Bagdassarov, N., Golabek, G.J., Solferino, G., Schmidt, M.W., Constraints on the Fe-S melt connectivity in mantle silicates from electrical impedance measurements, *Physics of the Earth and Planetary Interiors* (2008), doi:10.1016/j.pepi.2009.08.003

Constraints on the Fe-S melt connectivity in mantle silicates from electrical impedance measurements

Bagdassarov N.[*,1,2], *Golabek G. J.*[1,3], *Solferino G.*[2], *Schmidt M.W.*[2]

[*] Corresponding author

[1]Institute for Geosciences, Altenhöferallee 1,

University Frankfurt

D-60438 Frankfurt, Germany

[2]Institute for Mineralogy and Petrology,

Clausiusstrasse 25, ETH Zürich,

CH-8092 Zürich, Switzerland

[3] Institute for Geophysics,

Sonneggstrasse 5, ETH Zürich,

CH-8092 Zürich, Switzerland

Abstract

The connectivity of FeS-melts in olivine and in a fertile peridotite matrix has been addressed through in-situ electric impedance spectroscopy (IS) measurements at 1 GPa. A first series of experiments used sintered powder samples of a fertile peridotite xenolith mixed with 5-15 vol% $Fe_{70}S_{30}$ of eutectic composition. The sheared high-T garnet peridotite with Mg# ~ 0.90 is composed of 60 vol% olivine, 15% orthopyroxene, 5.3 % clinopyroxene and 19% garnet, the powder grain size was 20-30 μm, similar to the one employed by Yoshino et al. [2004]. For a second series, San Carlos olivine aggregates were used as solid matrix and 10-20 vol.% of eutectic $Fe_{70}S_{30}$ were added. For these, the average grain size was 3 μm, much smaller than in the experiments by Yoshino et al. [2003]. The powder mixtures of peridotite + $Fe_{70}S_{30}$ and olivine aggregates + $Fe_{70}S_{30}$ were first annealed for 2-5 days in a conventional piston-cylinder at 1 GPa and 950-970 °C. The electrical conductivity of samples has been measured using the impedance spectroscopy method in a BN-graphite-CaF_2 pressure cell with concentric cylindrical electrodes made from Mo- or Re-foil (which corresponds to an oxygen fugacity close to the IW buffer). The results indicate that up to 15 vol% of $Fe_{70}S_{30}$ the melt phase does not built a stable interconnected network in a peridotite matrix, as was recently indicated by Walte et al. [2007]. The percolation threshold for a stable FeS network in olivine matrix lies at 17.5 vol%, much higher the 6 vol% found by Yoshino et al. [2003]. Our result is in line with the high dihedral angles of typically 70-100^o for Fe-S melts in mantle materials. The higher interconnectivity threshold of this study, as compared to previous studies [Yoshino et al. 2003, 2004; Roberts et al., 2007] is a result of our smaller starting grain sizes (for olivine) in combination with much longer run durations. Both these experimental conditions result in enhanced grain growth and thus to a higher degree of textural equilibration, leading to the occurrence of the time depending pinging off of Fe-S melt films in our texturally more mature experiments.

Key words: *Earth's core, segregation, sulphide melt, olivine, peridotite*

Introduction

Current knowledge indicates that planetary accretion and differentiation procede simultaneously [e.g. Chambers, 2004]. Numerical modelling and laboratory investigations indicate that early formed planetesimals might have experienced significant or even total melting due to the decay of the short-lived radioactive isotopes ^{26}Al and ^{60}Fe [Merk et al., 2002; Greenwood et al., 2005; Hevey and Sanders, 2006; Sahijpal et al., 2007;]. During planetary growth, kilometre-sized bodies can be formed within ~10^4 *a,* and planetary embryos may reach the size of Mars within 0.1 –10 Ma [Chambers, 2004], thus being able to retain the radioactive heat from the short-lived, now extinct radionuclides. As pointed out by Terasaki et al. [2008], percolation of the iron-rich material might be initiated when temperatures become high enough to partially melt the iron alloy inside planetesimals. Percolation of Fe-S melt in a solid silicate matrix becomes the first possible core formation process during accretion and concomitant warming of the planetesimal. This segregation process will, with increasing temperature, be followed by Fe-S melt percolation in a partially molten, but grain supported peridotite mantle, and then by segregation of immiscible metal and silicate liquids in a magma ocean [e.g. Stevenson, 1990]. Percolation of Fe-S melt in a solid silicate matrix may contribute and influence the timing of metal core formation in early formed planetesimals. However, its efficiency will depend on the percolation threshold in the respective matrix material. This factor is dependent on the dihedral angle θ formed between the silicates and the iron alloy. The dihedral angle can be defined as

$$\Theta = 2\cos^{-1}\left(\frac{\gamma_{ss}}{2\gamma_{sl}}\right) \qquad (1),$$

where γ_{ss} and γ_{sl} are the interfacial energies per unit area of the solid–solid and solid–liquid interfaces, respectively [*e. g.* Laport and Provost, 2000].

If the dihedral angle is below 60°, no interconnection threshold exists and melt can be interconnected also when very small amounts of melt are available. If the dihedral angle is above 60°, then a certain percolation threshold has to be exceeded to enable interconnection. High surface tensions γ_{sl} of sulfide melts (ca. 500 J/m²) [Mungall and Su, 2005] lead to high wetting angle values typically ranging from 70-100° in the olivine + Fe-S system in static experiments [*e.g.* Ballhaus and Ellis, 1996; Minarik et al., 1996]. Although

Terasaki et al. [2008] showed that for high oxygen fugacities the dihedral angle may drop to 60°, these conditions are not thought to be common during the early formation of planetesimals [e.g. Wood and Halliday, 2005].

If the percolation threshold is low, percolation can contribute to inefficient core formation in the temperature range between Fe-S melting and silicate solidus, nevertheless, an amount of iron melt at the level of the percolation threshold will remain stranded in the matrix. A low percolation threshold of 6 vol% was derived by Yoshino et al. [2003] from electrical conductivity measurements for Fe-S melt in an olivine matrix. Such a threshold was also found by Roberts et al. [2007] in static annealing experiments. A similar value, about 5 vol% of iron melt has been suggested for the percolation threshold in a solid peridotite matrix [Yoshino et al., 2004], but the experimental conductivity measurements in Yoshino et al. [2004] do only sustain interconnectivity at 12 vol%. If these thresholds are correct, the percolation of FeS in mantle silicates is effective and the short time scale of the metal core formation in early formed planetesimals like Vesta can be explained by this segregation mechanism [Kleine et al., 2002; Yoshino et al., 2003, 2004].

Recently, these results have been addressed theoretically and experimentally by Walte et al. [2007] and their results and conclusions explicitly demonstrated that an interconnected network of Fe-S melt in unmolten silicates can not be stable at low melt fractions and pinches off in long term experiments. Walte et al. [2007] concluded that the steady state textural equilibrium of Fe-S melt possessing a high wetting angle may only be in a form of isolated droplets and that in order to form a stable melt network, a percolation threshold of 10-15 vol% must be overcome. If a stable interconnection of Fe-S melt in a silicate matrix is possible only at high volume fractions, other mechanisms of metallic sulfide segregation should be taken into consideration. As far as only isolated melt pockets of Fe-S can form under these conditions in a solid silicate matrix, the mobility of these droplets is quite restricted, because they collect in triple junctions, grow in size and may not be able to pass though a throat of intergrain capillaries [Mungall and Su, 2005]. Thus, only at high degrees of partial melting a mobility of FeS-melt is possible in mantle silicates, at the extreme, this leads to the rainfall mechanism of iron droplet sinking in a completely molten magma ocean [Stevenson, 1990; Rubie et al, 2003; Rubie et al., 2007; Höink et al., 2006]. Additionally, the non-hydrostatic deformation of mantle material, which causes the development of a strong melt-

preferred orientation [Bruhn et al., 2000; Hustoft and Kohlstedt, 2006; Groebner and Kohlstedt, 2006] may also be a viable intermediate temperature core formation mechanism.

In this work we tested the long-term stability of connectivity of Fe-S melt in a peridotite (run series 1) and a olivine matrix (run series 2) by measuring the electrical resistance of pre-sintered samples of olivine and fertile peridotite with varying volume contents of eutectic Fe-S melt. These experiments were essentially similar in their setup to the experiments performed by Yoshino et al. [2003, 2004], except for a different electrode-sample geometry which allows to measure electrical resistivities down to the conductivities of the olivine matrix.

Experimental setup

Sample preparation

The starting material used for series 1 experiments were mixtures of natural fertile garnet peridotite from a xenolith of the Jericho kimberlite, Northern Territories, Canada (for details see Kopylova and Russell, [2000]) and an eutectic composition of Fe-S. The equilibration of the xenolith occurred at T=1,190-1,260 °C and 5.85-5.95 GPa according to different geothermobarometers. The relative oxygen fugacity of equilibration has been estimated as $\Delta\log(f_{O2})$=-3.2, the $Fe^{3+}/\Sigma Fe$ in garnet is 0.107 [McCammon and Kopylova, 2004] and the bulk Mg# is 0.896. The xenolith consists of 60 vol% olivine, 15 vol% orthopyroxene, 5.3 vol% clinopyroxene and 19.7 vol% garnet. The peridotite was crushed and then milled in a silicon-nitride mortar, to get a powder with a grain size of about 20-30 µm, similar to the one used by Yoshino et al. [2004]. The grain size distribution of powders has been measured with a laser particle analyzer, the Mastersizer 2000 (Malvern Instrument Ltd.). The $Fe_{70}S_{30}$ (weight %) composition of the iron-sulfide powder is that of the eutectic of the Fe-FeS system at 1 GPa [Brett and Bell, 1969] and has been prepared from Fe and FeS chemicals (99,99% ChemPu ®).

Starting material for series 2 experiments were natural San Carlos olivine and synthetic Fe and S powders. Olivine powder was prepared by crushing and milling under ethanol for 2-3 h. The final grain size

was measured with the use of laser diffraction using the Mastersizer 2000. The grain size distribution indicate an average grain size of 1.8 μm, a maximum size of 10 μm and 90% of grains were between 0.6 μm and 4.3 μm, a grain size much finer than the one employed by Yoshino et al. [2003]. Pieces of sulfur (99.999% purity, chips of 6 mm, Ceram^{TM} Inc.) were crushed and milled manually in an agate mortar and then mixed with iron powder (99.9% purity, powder with mesh 5 μm Ceram^{TM} Inc.). The exact composition of this iron sulfide powder is 70.5 wt.% Fe and 29.5 wt.% of S, but will be further also referred to as $Fe_{70}S_{30}$.

For both run series, the Fe-S or Fe-FeS powders (later on both will be referred to as Fe-S) were pressed into pellets and sealed in evacuated quartz tubes at 10^2 Pa. These tubes were kept at 1200 °C over 5 h in a vertical furnace and then quenched in water. Then the pellets were crushed and milled under ethanol over 10 min. The final mixtures were prepared from powders of fertile peridotite or olivine and the Fe-S composition in proportions of 5-20 vol% of $Fe_{70}S_{30}$ by grounding under ethanol. The dried mixtures were agitated over 10 min to get a maximum of homogenization, then dried in air and stored under vacuum.

Electrical impedance measurements

In-situ electrical conductivity measurements for both series have been performed in an end-loaded piston cylinder press connected with a Solatron^{TM} 1260 Phase-Gain-Analyzer. A 1-V sine signal in the frequency range from 0.01 Hz to 100 kHz was applied to the sample, to measure electrical impedance by using a 2-points method. The measuring cell consisted of a coaxial cylindrical capacitor with two electrodes from pure Re or Mo foil (0.05 mm in thickness, 99.9% purity). The losses of Fe-S in Re are negligible even when Fe-S droplets are in contact with Re-foil [O'Neill and Mavrogenes, 2002]. The diameters of the outer and inner electrodes were 3.9 mm and 2.1 mm, respectively. The geometric factor of the electrodes has been varied from 3.5 to 6 cm, depending on the length of the electrodes. The electrical resistance of samples could be measured in this coaxial cylindrical geometry in the range of 1 Ω to 100 MΩ [Bagdassarov et al., 2001; Maumus et al., 2005]. The starting material was placed and pressed between the two electrodes. The maximum run conditions were 1080-1320 °C and 1 GPa for series 1 runs and 1050-1150 °C and 1 GPa for series 2 runs. The following procedure has been applied for both run series: The

samples were heated at 1 GPa and temperatures just below the eutectic melting point of Fe-FeS (about 970 °C; [Brett and Bell, 1969]). These pressure and temperature conditions were then kept for 70-75 h. Afterwards, the temperature was increased stepwise with increments of about 10-12 °C and after each temperature step, conditions were maintained for about 3 h. After reaching the maximum temperature, the samples were cooled down stepwise to 850-900 °C, and kept there for over 12 h. For the peridotite + Fe-S samples, a second and third heating-cooling cycle was performed. After the first heating cycle, the olivine + Fe-S samples were annealed for ≥ 72 h at the highest temperature before the subsequent heating cycle, only sample OV-FS-1 was not annealed below the melting point of Fe-S and temperature was increased directly to 1110 °C.

The typical results of electrical conductivity and resistance spectra are presented in Fig. 1 and 2. The bulk resistance and conductivity were estimated from Argand-plots, a plot of imaginary against real component of electrical impedance measured at varying frequencies. The fitting procedure of impedance spectra has been already described elsewhere [e.g. Maumus et al., 2005]. In the case when FeS built an interconnected network, the spectra of electrical conductivity in Argand plots represent vertical lines (see filled symbols in Fig. 1) and demonstrate non dependence on frequency (Fig. 2). When there was no interconnected Fe-S network in a sample, the conductivity of the sample has been determined by the electric properties of the silicate matrix. During the process of Fe-S network interruption, a new arc develops in the low frequency region of Argand plots (open symbols in Fig. 1). After finishing the experiments, the samples were cut along the axis of the coaxial cylinders and polished section were imaged with backscattered electrons in a microprobe analyzer (JEOL JXA 8200), at the same time, wavelength distributions analyzes (WDS) were made on each sample. The change in the geometric factor after experiments did not exceed 2-3%. Microprobe analysis and x-ray mapping at the contact between the electrode and the sample did not reveal any contamination of electrode material by the Fe-S phase, and neither Re or Mo diffusion into the Fe-S alloy (see Fig. 3 (*a*) and (*b*)).

Results

Our bulk electrical conductivities measured in-situ in peridotite + Fe-S and olivine + Fe-S aggregates are shown in Figs. 4 and 5, respectively. Below the melting point of Fe-S and during the annealing phase, conductivities vary negligibly with temperature and activation energies are within error 0 eV. The measured conductivities at subsolidus temperatures correspond to the conductivity of Fe-S films situated in intergranular space. The latter determine the overall conductivity of the aggregates as long as a continuous network of Fe-S exists. At temperatures slightly above the melting point of Fe-S (ca. 985 °C) a sudden jump to lower conductivities is observed in all samples except those with ≥17.5 vol% $Fe_{70}S_{30}$. During successive heating and cooling cycles, this lower electrical conductivity exhibits an activation energy typical for fertile peridotites (1.54 eV, Fig. 7 in [Bagdassarov et al., 2007]) in series 1, or typical for San Carlos olivine close to the IW-buffer [Constable, 2006] in series 2. This can only be explained due to the absence of connectivity for the iron-sulfide phase. The conductivities measured after the drop in electrical conductivity are in good agreement with results for olivine conductivity from Xu et al. [1998] and Schock et al. [1989], and with the theoretical model for the dry olivine SEO3 proposed by Constable [2006].

The experiment with 17.5 vol% Fe-S in the olivine aggregate maintains a stable high electrical conductivity over 94 h at temperatures above the Fe-S melting point, and the values of conductivity correspond to the case of interconnected Fe-S. Upon cooling, this experiment yields a significant drop in conductivity, but conductivities remain several orders of magnitude above the conductivity of the olivine aggregates (Fig. 5). The experiment with 20 vol% Fe-S remains during the entire heating, dwell and cooling periods at high conductivities typical for Fe-S, maintaining interconnectivity throughout the entire experiment. All peridotite plus $Fe_{70}S_{30}$ samples show reversible conductivities after the drop during repeated heated cooling cycles. We conclude that stable interconnectivity is achieved between 15 and 17.5 vol% of Fe-S melt, a result in considerable contrast to Yoshino et al. [2003, 2004].

Image analysis of the run products of the olivine + Fe-S system confirms that the post-experiment melt fraction is within error (typically 0.5-1.0 vol%) identical to the one of the starting material; with the exception of run OV-FS-1 which has not been annealed in the subsolidus, shows larger heterogeneities, and

thus has been repeated (Table 1). The variation of Fe-S composition before and after experiments was negligible (Table 2). For both run materials, we see no rise in the electrical conductivity in the temperature range below the Fe-S solidus for Fe-S fractions as large as 15 vol% FeS (Fig. 4+5), which is in disagreement with results from Yoshino et al. [2004]. Optical analysis reveals the development of beads-on-string-structures of Fe-S melt inclusions due to the high interfacial energy between Fe-S melts and the silicates, which explains the drop in the electrical conductivity.

Finally, it should be noted, that the absolute values of electrical conductivity in samples in which Fe-S is still building an interconnected network cannot be measured precisely because the resistance of Fe-S is much smaller than the resistance of Mo- or Re-foil electrodes themselves.

Discussion:

Our electrical impedance measurements demonstrate that the interconnection threshold for stable networks in a peridotite matrix lies above 15 vol% Fe-S melt and at 15-17.5 vol% in an olivine matrix. The activation energies (Fig. 6) and impedance spectra (Fig.1) indicate the disruptive character of the Fe-S phase connectivity at T > 985 °C and $Fe_{70}S_{30}$ contents < 17.5 vol%. Below 985 °C, the electrical conductivity is frequency independent as characteristic for metals (Fig. 2). The conductivity of peridotite samples with 5, 7.5, 10, and 15 vol% of Fe-S melt drops from values of 0.1 S/m to typically 10^{-3} S/m at temperatures between 985 and 1020 °C, i.e. the interconnectivity of Fe-S is not stable with time at temperatures above the melting temperature of Fe-S.

Figure 4 shows that only the peridotite sample with 15 vol% of Fe-S exhibits a two step drop of conductivity during annealing. The second drop occurs at ca. 1080 °C and the end value of conductivity is $3 \cdot 10^{-5}$ S/m, lower than the conductivity of San Carlos olivine at oxygen fugacities of the IW-buffer after Constable [2006]. This low conductivity implicates that this large amount of Fe-S added to the fertile peridotite causes extremely reduced conditions which change the conductivity of the sample itself. By adding progressively from 5 to 15 vol% of Fe-S the overall conductivity of fertile peridotite decreases (see Fig. 4). Fig. 5 summarizes the results from the olivine + Fe-S samples, characteristic conductivity drops occur from typically 0.05 S/m to 10^{-3} S/m, again at temperatures between 985 and 1020 °C. The

characteristic time of this drop is 0.5-1 h. After this conductivity drop, activation energies correspond to those of peridotite or olivine, clearly demonstrating the transition from electrical conduction through a Fe-S network to conduction through a silicate matrix. The most plausible explanation for the sudden conductivity drop is the disruption of the network after the melting of Fe-S, which results in separation of melt into isolated pockets. The initially observed high conductivities in both series should be due to the presence of thin iron-sulfide films surrounding the silicate grains. This is possible because of the much smaller stiffness of FeS (relative hardness 3.5-4) in comparison to olivine (relative hardness 6.5-7), such that the highly deformable and plastic FeS is able to fill gaps during cooling of the starting material. These films then disrupt during melting of the alloy.

Above the melting temperature of Fe-S, the molten phase possesses a high dihedral angle (larger than 70°) with olivines, pyroxenes, spinel, and garnet [Gaetani and Grove 1999, Terasaki et al., 2007], in perfect agreement with our finding that melt fractions > 15 vol% are necessary to achieve interconnectivity in texturally mature aggregates. Terasaki et al. [2008] also determined dihedral angles between olivines with Mg# 0.9-0.76 and Fe-S melt at oxidizing conditions. In agreement with Gaetani and Grove [1999] and Rose and Brenan [2001], large oxygen concentrations of about 15-25 at.% in combination with low pressures were found to be necessary to obtain Fe-S melt wetting angles of less than 60°. Both conditions do not apply to our or Yoshino et al.'s [2003, 2004] experiments.

From their measurements of electrical conductivity in peridotite + Fe-S and olivine + Fe-S melt, Yoshino et al. [2003, 2004] concluded that the initial interconnectivity of molten Fe-S persists even when only 6 vol.% of Fe-S melt is present in the silicate matrix. In Yoshino et al. [2003, 2004], the first and subsequent second and third heating-cooling cycles provide very different electrical conductivities and activation energies of the bulk electric properties of the material. This can be only explained by a non-stationary melt distribution. Close examination of the experimental protocol reveals, apart from the different electrode geometry, three substantially different aspects: run times, starting grain sizes, and the use of boron nitride (BN) sleeves in Yoshino et al.'s experiments. The latter is unlikely to directly influence the Fe-S melt distribution or connectivity threshold, as both the presence of graphite (as a heater in the piston cylinder assembly) and/or BN results in oxygen fugacities at which the solubility of oxygen is

negligible in Fe-S alloys [Gaetani and Grove, 1999]. However, both starting grain size and run time may have decisive effects on the melt distribution. Walte et al. [2007] demonstrated that the disruption of films of melts which possess a high dihedral angle occurs with time during grain growth. In particular, Walte et al. [2007] observed, that melt previously distributed along interconnected channels becomes, with increasing annealing time, stuck in isolated melt pockets as smaller grains disappear in favour of growing larger grains.

The disruption of the Fe-S melt network occurs in our olivine + Fe-S experiments after 65-80 h, a time span similar to the olivine + Fe-S experiments of Yoshino et al. [2003]. However, our starting olivine grain size of 1.8 μm is much smaller than the 10-20 μm of Yoshino et al. [2003], which leads to significantly enhanced grain growth. Our resulting grain sizes of typically 10 μm are equivalent to the disappearance of > 99% of the grains initially present, and thus a much more effective pinging off of Fe-S melt channels occurs in our setup. We conclude that for reaching an equivalent degree of textural equilibration and thus shutdown of the Fe-S interconnectivity, much longer run times would have been necessary in the experiments of Yoshino et al. [2003] on relatively coarse grained olivine. Similarly, the 24 h synthesis time of olivine + Fe-S aggregates by Roberts et al. [2007] are insufficient for textural maturation, as already suggested by Walte et al. [2007].

Yoshino et al. [2003, 2004] employed a parallel plate geometry for the measuring electric cell including a BN sleeve around the sample. This latter is connected to the electrodes in parallel to the sample and inhibits measurement of resistivities down to those of an olivine or peridotite matrix, as the shunt resistance of the BN sleeve is much lower than for any silicate agglomerate. Thus, the background conductivity of Yoshino et al. [2003, 2004] corresponds to their BN sleeve for temperatures above ca. 500 ^{o}C. In contrast, in our experiments, a coaxial cylindrical capacity cell capable to measure silicate aggregate resistivities (down to 1 Ω) has been used. At the melting temperature of the Fe-S alloy (1000 ^{o}C), conductivities for the samples with 0, 3, and 6 vol% Fe-S melt in the peridotite matrix were lower than the background conductivity of Yoshino et al. [2004], while at 12, 18, and 26 vol% conductivities were several orders of magnitude larger than the BN-background. A straightforward conclusion would be to interpret the 12 vol% conductivity as yielding the beginning of interconnectivity. Nevertheless, at subsolidus conditions (600-800 ^{o}C) the 6 vol% experiment showed that the conductivity slightly increased against the BN-background,

which Yoshino et al. [2003] interpreted as indicative for interconnectivity. We do not follow this argument, as above the Fe-S melting temperature the peridotite-metal agglomerate did not show metal conductivities but those of the BN-sleeve and thus characteristic for silicate aggregates. We interpret the Yoshino et al. [2004] experiments as yielding interconnectivity at or slightly below 12 vol%, still somewhat lower than the 15 vol% at which connectivity still drops to peridotite matrix values in our experiments. The most likely explanation for this discrepancy lies in insufficient run times in Yoshino et al. [2004]. In our experiment at 15 vol% Fe-S, 135 h were necessary to observe the conductivity drop (total run time 194 h, Table 1), but Yoshino et al. held temperatures only for 84 hours in the experiment with 12 vol% Fe-S.

The time dependence of the textural equilibration process is also illustrated by the fact, that the shift from metal to olivine conductivity after melting always took a few hours to be accomplished. The reduction of conductivity did not result from melt escape from the olivine matrix, as the pre-annealed samples conserve their metal melt fraction (Table 1). This behavior indicates that the connected Fe-S network remains as a transient stage for a few hours even after melting of Fe-S, until textural maturation eventually disrupts the network, as monitored by the electrical conductivity dropping from metal values to olivine values. The migration of Fe-S melt into isolated pockets is driven by the high surface tension of the metal alloy, which yields a 'negative diffusion' of the metal melt itself [Jurewicz and Watson, 1985; Stevenson, 1990]. In this sense, a more realistic percolation threshold was determined in the present study.

Conclusions:

The main conclusion of the present study reiterates that Fe-S melts have high connectivity thresholds in peridotite or olivine aggregates. This experimental result is in agreement with theoretical and experimental work (e.g. Walte et al. [2007]), which sustains that in a matrix-melt systems with high dihedral angles (> 60°) such as peridotite or olivine + Fe-S an interconnectivity of the melt phase is unstable at low amounts of Fe-S melt. Our experimental results are not in direct conflict with the experimental observations of Yoshino et al. [2003, 2004] and Roberts et al. [2007], but lead to contradicting interpretations. Due to shorter run times and larger starting grain sizes, the latter studies have not achieved the same textural maturation as in our experiments, and the interconnectivity observed in these studies has to be considered

as transitional. The threshold and thus melt fraction for stable percolation in an olivine + Fe-S system is around 17.5 vol% of Fe-S and above 15 vol% of Fe-S in peridotite + Fe-S. Our results therefore exclude an efficient core formation process in unmolten peridotite at metal fractions characteristic for the terrestrial planets. Alternative core forming processes such as the rainfall mechanism in magma oceans [Stevenson, 1990; Rubie et al., 2003; Rubie et al., 2007; Höink et al., 2006] or Fe-S melt segregation in partially molten peridotite are thus necessary for differentiation processes in early formed planetesimals.

Acknowledgements:

We thank Nico Walte and an anonymous reviewer for their valuable comments, which helped to improve the manuscript significantly.

References:

- Bagdassarov N., Freiheit C.-H., Putnis A., 2001. Electrical conductivity and pressure dependence of trigonal-to-cubic phase transition in lithium sodium sulphate. *Solid State Ionics* 143, 285-296.
- Bagdassarov N., Kopylova M., Eichert S., 2007. Laboratory derived constraints on electrical conductivity beneath Slave craton. *Phys. Earth Planet. Int.* 161, 126-133, doi:10.1016/j.pepi.2007.01.001.
- Ballhaus, Ch. and D. J. Ellis, 1996. Mobility of core melts during Earth's accretion. *Earth Planet. Sci. Lett*. 143, 137-145.
- Brett R. and P.M. Bell, 1969. Melting relations in the Fe-rich portion of the system Fe-FeS at 30 kb pressure. *Earth Planet. Sci. Lett*. 6, 479-482.
- Bruhn D., Groebner, N. and D. L. Kohlstedt ,2000. An interconnected network of core forming melts produced by shear deformation. *Nature* 403, 883-886.
- Chambers J. E., 2004. Planetary accretion in the inner Solar System. *Earth. Planet. Sci. Lett*. 223, 241-252, doi:10.1016/j.epsl.2004.04.031
- Constable S. 2006. SEO3: A new model of olivine electrical conductivity, *Geophys. J. Int.* 166, 435–437, doi: 10.1111/j.1365-246X.2006.03041.x.

- Groebner, N. & D.L. Kohlstedt, 2006. Deformation-induced metal melt networks in silicates, Implications for core-mantle interactions in planetary bodies, *Earth Planet. Sci. Lett.* 245, 571-580, doi:10.1016/j.epsl.2006.03.029.
- Greenwood R. C., Franchi I.A., Jambon A. and P.C. Buchanan, 2005. Widespread magma oceans on asteroidal bodies in the early solar system. *Nature* 435, 916-918, doi:10.1038/nature03612.
- P.J. Hevey & I.S. Sanders, 2006. A model for planetesimal meltdown by ^{26}Al and its implications for meteorite parent bodies, M*eteoritics & Planetary Science* 41, 95–106.
- Höink T., J. Schmalzl and U. Hansen, 2006. Dynamics of metal-silicate separation in a terrestrial magma ocean, *Geochem. Geophys. Geosyst.* 7, Q09008, doi:10.1029/2006GC001268.
- Hustoft, J.W. and D.L. Kohlstedt, 2006. Metal-silicate segregation in deforming dunitic rocks, *Geochem. Geophys. Geosyst.* 7, Q02001, doi:10.1029/2005GC001048.
- Kopylova M. G., Russell J. K., 2000. Chemical stratification of cratonic lithosphere: constraints from Northern Slave Craton, Canada. *Earth Planet. Sci. Lett.* 181, 71-87.
- Kleine T., Münker C., Mezger K., Palme H., 2002. Rapid accretion and early core formation on asteroids and the terrestrial planets from Hf-W chronometry. *Nature* 418, 952-955, doi:10.1038/nature00982.
- Laport D., Provost A., 2000. The grain scale distribution of silicate, carbonate and metallsulfide partial melts: a review of theory and experiments. In: Bagdassarov N., Laport D. and A Thompson (eds.) Physics and Chemistry of Partially Molten Rocks, Kluwer Academic Publishers, Dordrecht, pp.93-140.
- Maumus J., Bagdassarov N. and H. Schmeling, 2005. Electrical conductivity and partial melting of mafic rocks under pressure. *Geochim. Cosmochim. Acta 69*, 4703-4718, doi:10.1016/j.gca.2005.05.010.
- McCammon C., Kopylova M. G., 2004. A redox profile of the Slave mantle and oxygen fugacity control in the cratonic mantle. *Contrib. Mineral. Petrol*. 148, 55-68, doi:10.1007/s00410-004-0583-1.
- Merk R., Breuer D., Spohn T., 2002. Numerical modeling of ^{26}Al-induced radioactive melting of asteroids considering accretion, *Icarus* 159, 183-191, doi:10.1006/icar.2002.6872.
- Minarik W. G., Ryerson F. J., Watson E. B., 1996. Textural entrapment of core-forming melts. *Science* 272, 530-533.

- Mungall J. E., Su Sh., 2005. Interfacial tension between magmatic sulphide and silicate liquids: Constraints on kinetics of sulphide liquation and sulphide migration through silicate rocks. *Earth Planet. Sci. Lett.* 234, 135-149, doi:10.1016/j.epsl.2005.02.035.
- O'Neill H. St. C., Mavrogenes J. A., 2002. The sulphide capacity and the sulphur content at sulphide saturation of silicate melt at 1400°C and 1 bar. *J. Petrol.* 43, 1049-1087.
- Roberts J. J., Kinney J. H., Siebert J., Ryerson F. J., 2007. Fe-Ni-S melt permeability in olivine: Implication for planetary core formation. *Geophys. Res. Lett.* 34, L14306, doi: 10.1029/2007GL030497.
- Rose L. A., and Brenan J. M., 2001. Wetting properties of Fe-Ni-Co-Cu-O-S melts against olivine: implications for sulfide melt mobility. *Economic Geology* 96, 145-157, doi: 10.2113/96.1.145
- Rubie D.C., Melosh H.J., Reid J.E., Liebske C., Righter K., 2003. Mechanisms of metal-silicate equilibration in the terrestrial magma ocean. *Earth Planet. Sci. Lett.* 205, 239-255.
- Rubie D. C., Nimmo F., Melosh H. J., 2007. Formation of Earth's core. In: D.J. Stevenson (ed.) *Treatise on Geophysics Vol. 9: Evolution of the Earth*,. Elsevier, Amsterdam, pp. 51-90.
- Sahijpal S., Soni, P., Gupta, G., Numerical simulations of the differentiation of accreting planetesimals with ^{26}Al and ^{60}Fe as heat sources, *Meteoritics & Planetary Sciences* 42, 1529-1548, 2007.
- Schock, R.N., Duba, A.G., Shankland T. J., 1989. Electrical conduction in olivine. *J.Geophys. Res.* 94, 5829-5839.
- Stevenson D. J., 1990. Fluid Dynamics of Core Formation. In: Newsom, H.E., Jones, J.H. (Eds.), *Origin of the Earth*, Oxford Univ. Press; Houston, pp. 231 -249.
- Terasaki H., Frost D. J., Rubie D. C., Langenhorst F., 2007. Interconnectivity of Fe-O-S liquid in polycrystalline silicate perovskite at lower mantle conditions. *Phys. Earth Planet. Int.* 161, 170-176, doi:10.1016/j.pepi.2007.01.011.
- Terasaki H., Frost D. J., Rubie D. C., Langenhorst F., 2008. Percolative core formation in planetesimals. *Earth Planet. Sci. Lett.* 237, 132-137, doi: 10.1016/j.epsl.2008.06.019
- Walte N. P., Becker J. K., Bons P. D., Rubie D. C., Frost D. J., 2007. Liquid-distribution and attainment of textural equilibrium in a partially-molten crystalline system with a high-dihedral-angle liquid phase. *Earth Planet. Sci. Lett.* 262, 517-532, doi:10.1016/j.epsl.2007.08.003.

- Xu, Y., B.T. Poe, T.J. Shankland, D.C. Rubie, 1998. Electrical conductivity of olivine, wadsleyite and ringwoodite under upper-mantle conditions, *Science* 280, 1415-1418.
- Yoshino T., Walter M. J., Katsura T., 2003. Core formation in planetesimals triggered by permeable flow. *Nature* 422, 154-157, doi:10.1038/nature01459.
- Yoshino T., Walter M. J., Katsura T., 2004. Connectivity of molten Fe alloy in peridotite based on in situ electrical conductivity measurements: implications for core formation in terrestrial planets. *Earth Planet. Sci. Lett.* 222, 625-643, doi:10.1016/j.epsl.2004.03.010.

Table 1. Annealing conditions and electrical conductivity measurements in San Carlos olivine aggregates and fertile peridotite + Fe-S melts.

Run	Peridotite or Olv/Fe-S ratio [vol %]	T_{max} in each cycle [°C]	Total duration [h]	Annealing time [d]	Electrical Conductivity at T_{max} of each cycle [S/m]	FeS-content after el.cond. experiment [vol %]	Activation energy [eV]	Electrical Conductivity at ca. 1080 °C [S/m]
P-1	95/5	1017/1080	152.3	3.2	$1.5x10^{-3}/5.0x10^{-2}$	n.d.	n.d/ 1.59±0.1	$3.5x10^{-3}/5.0x10^{-3}$
P-2	92.5/7.5	1207	122.4	1.8	$5.7x10^{-4}$	n.d.	2.04±0.1/1.85±0.1	$3.9x10^{-4}/8.3x10^{-5}/1.4x10^{-4}$
P-3	90/10	1080/1084	135.3	2.7	$3.0x10^{-4}/2.1x10^{-5}$	n.d.	2.3±0.1/1.87±0.1	$3.0x10^{-4}/2.6x10^{-5}$
P-4	85/15	1084/1088	194.1	4.8	$1.7x10^{-2}/ 2.5x10^{-5}$	n.d.	1.24 ± 0.1/ n.d.	$9.7x10^{-3}/2.5x10^{-5}$
OV-FS-1	90/10	1110	90	0	$2.46x10^{-2}$	6.0±1.5	-	$4.0x10^{-2}$
OV-FS-2	90/10	1150	92	2.7	$1.62x10^{-2}$	10.4±0.9	1.55±0.10	$2.0x10^{-2}$
OV-FS-4	80/20	1050	96	2.8	$2.65x10^{-2}$	19.8±1.3	0.06±0.04	$1.1x10^{-2}$
OV-FS-5	85/15	1080	150.3	2.7	$3.06x10^{-2}$	15.1±0.5	1.71±0.12	$3.1x10^{-2}$
OV-FS-6	82.5/17.5	1080	98	2.7	$1.1x10^{-2}$	17.5±0.5	1.45±0.10	$1.0x10^{-2}$

Numbers in the table separated with slash correspond to several consecutive heating cycles. Run OV-FS-3 is with the ratio of Ol/Fe-S is 80/20 is not mentioned in the table. The annealing time at temperature above 1000 °C is 72 h, the conductivity of the sample is the same as in the run OV-FS-4. The melt abundances estimated from BSE images are as follows: OV-FS-1 6.7 ± 1.4vol%, OV-FS-2 10.1 ± 1.0, OV-FS-4 20.1 ± 1.4, OV-FS-5 15.8 ± 0.8. For sample OV-FS-6, Fe-S melt phase is not perfectly homogeneously distributed. The region in the cylindrical gap between inner and outer electrodes contains 18.3 ± 1.0, whereas, the area below the inner electrode contains 16.8 ± 0.9. In peridotite samples the estimated Fe-S abundances after electrical conductivity experiments are as follows: in P-1 4.6±0.8 vol%, in P-2 7.3±0.9.

TABLE 2

Composition of olivines and iron-sulfide alloys after annealing

Runs with olivine plus iron-sulfide mixtures

Oxide (weight %)	OFS-1	OFS-2	OFS-4	OFS-5	S. Carlos
SiO2	39.91	39.97	40.73	39.63	40.99
MgO	49.08	48.86	49.06	49.49	49.81
FeO	11.32	11.22	10.83	10.73	8.96
MnO	0.10	0.11	0.12	0.11	0.23
total	100.41	100.15	100.75	99.96	
# of analysis	15	16	8	30	

Runs with iron-sulfide mix

Element (weight %)	FS-1	FS-2
Fe	66.44	67.96
S	29.36	30.46
O	0.51	0.80
total	96.31	99.22
# of analysis	18	12

Table 3.					
Chemical analyses	of Fe-S melts	in peridotite	samples after	annealing	
sample	P-1	P-2	P-3	P-4	
Fe	62.40	62.27	62.36	62.33	
S	37.44	37.86	37.09	36.97	
O	0.00	0.00	0.00	0.00	
total	99.84	100.13	99.45	99.30	

The estimations of dihedral angle from BSE images of samples after electrical conductivity experiments are as follows: for P-1 101°, P-2 100°, P-3 103°, P-4 98°.

Table 4.							
Chemical analyses	of silicate phases	in peridotite	samples				
after electrical	conductivity	experiments					
Phase	olivine - core	olivine - rim	Opx	Garnet	Cpx	Sp	
SiO2	39.98	39.13	56.87	41.38	53.26	0.16	
TiO2	0.01	0.02	0.07	0.44	0.16	0.20	
Cr2O3	0.05	0.09	0.30	4.63	1.07	16.98	
Al2O3	0.02	0.06	0.65	19.22	2.58	50.57	
FeO	9.65	14.52	5.93	8.29	3.91	11.11	
MnO	0.12	0.15	0.13	0.34	0.12	0.17	
NiO	0.35	0.15	0.11	0.01	0.04	0.01	
MgO	49.14	45.45	34.08	20.06	17.49	20.49	
CaO	0.05	0.11	0.80	4.91	18.94	0.07	
Na2O	0.02	0.01	0.18	0.05	1.18	0.00	
K2O	0.00	0.00	0.00	0.00	0.03	0.00	
total	99.41	99.69	99.13	99.33	98.78	99.75	
Mg#	89.5*	84.2*	0,91*	0,81*	0,88*	90.5*	
*Fe total							

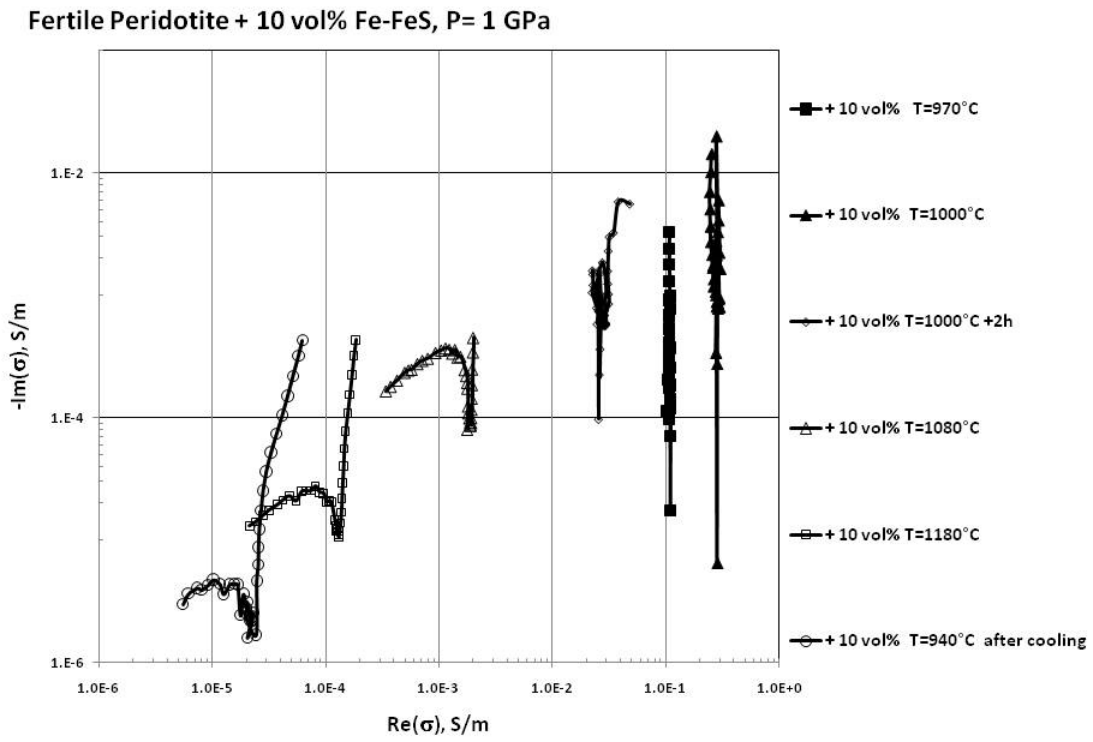

Fig. 1. Impedance spectra measured in fertile peridotite with 10 vol% of Fe-S. At temperatures below the melting point o*f Fe-S (*<985 °C) the *spectra* indicate a pure metallic character of the electrical conductivity without frequency dependence (filled symbols). This situation corresponds to an interconnected network of Fe-S in the aggregate. During annealing and at high temperatures the spectra are typical for silicates with the developed arcs and frequency dependence of the electrical conductivity. After cooling below 1000 °C the type of spectra does not change. Left shoulder of spectra corresponds to lower frequency.

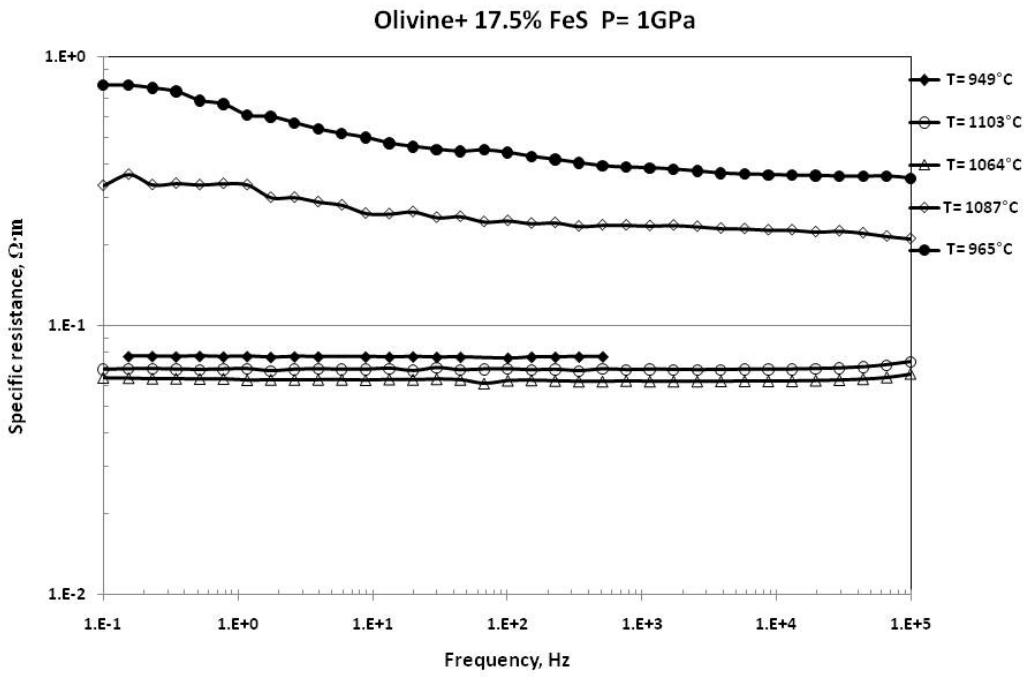

Fig. 2. Specific resistance spectra of San Carlos olivine with 17.5 vol % of Fe-S. During annealing from 949 °C to 1103 °C during the first 72 h the resistance is of a pure metallic character. By further annealing and cooling below 985 °C the resistivity increases by 1 order of magnitude but still corresponds to a continuous network of Fe-S melt in the sample.

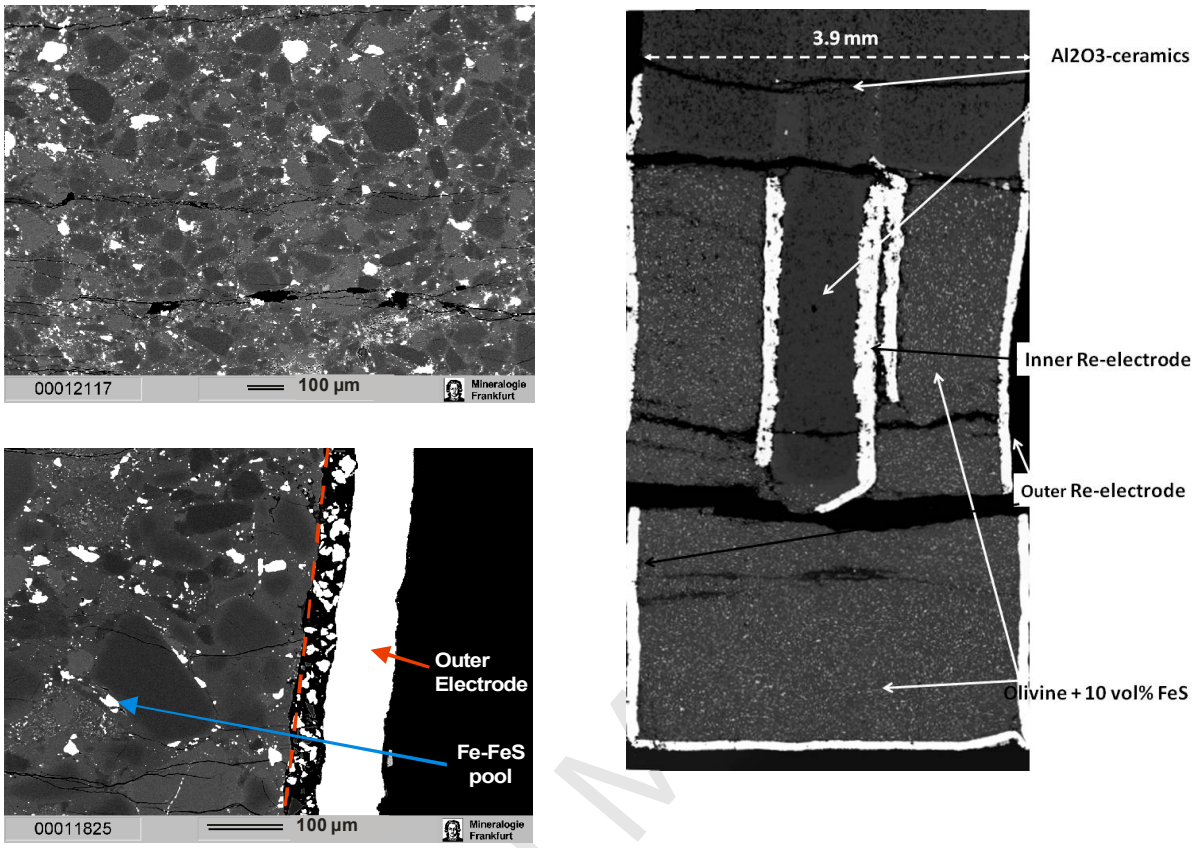

Fig. 3(a): (left upper and lower panels) Sample of peridotite with initial 10 (upper left panel) and 5 (bottom left panel) vol % of iron sulfide after electrical conductivity experiment at 1 GPa and with T_{max}=1084 °C and 1240 °C. respectively. Iron sulfide pools are white, olivine grains are dark grey, pyroxenes are grey, clinopyroxenes are light grey. (left lower panel) On the left side of the photo is the area near a Re-electrode. EDS analysis of metal electrode does not reveal any contamination with Fe, S or O. (The extended contact zone between electrode and the sample in the left panel is a result of polishing and contains pieces of Re). (right panel) Right photo represents the sample OV-FS-2 (Table 1) in the coaxial cylindrical cell after the IS measurements. The cut is not exactly along the cylindrical axe. The thermocouple was in contact with the inner electrode during experiment.

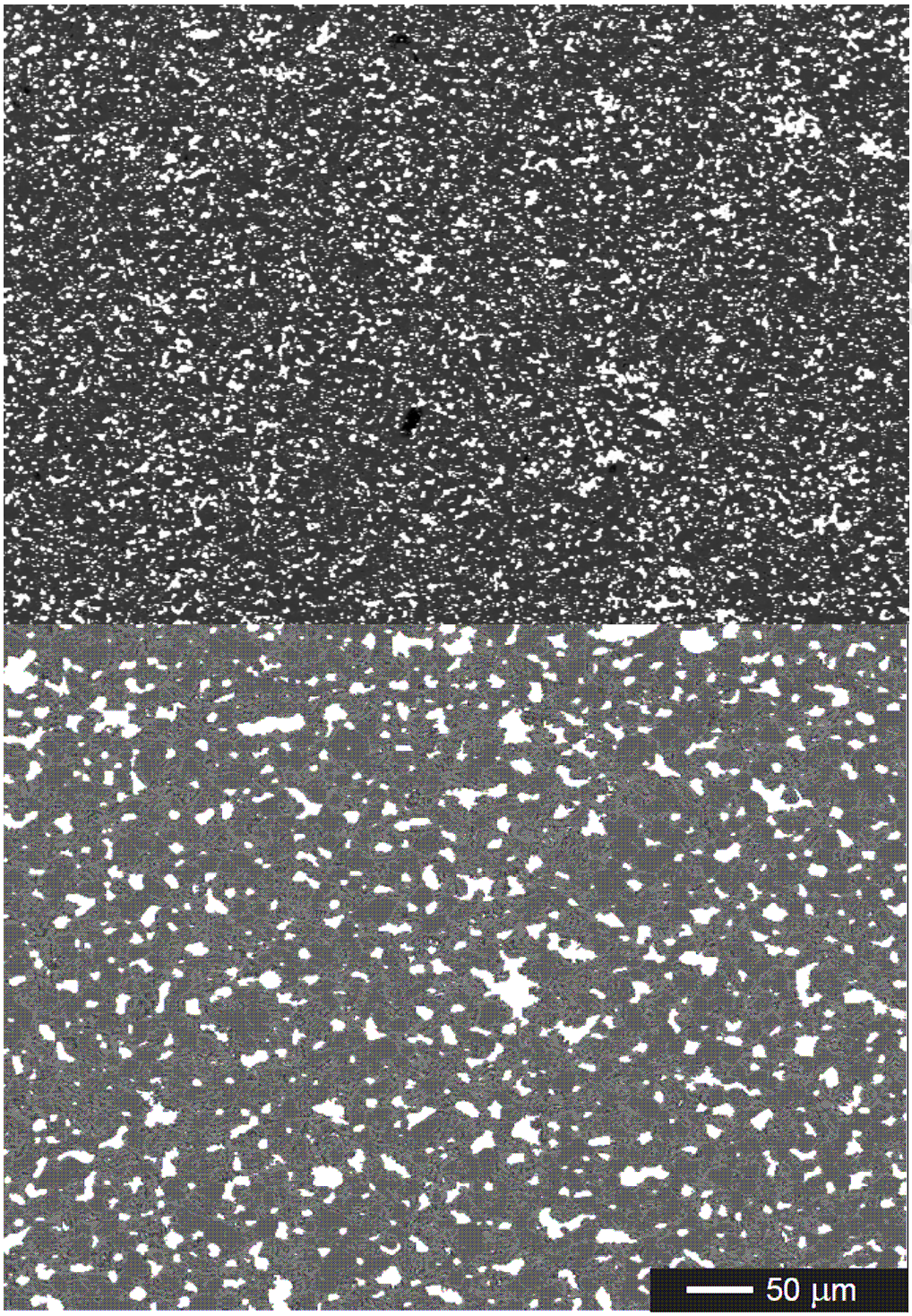

Fig. 3(*b*). Upper panel: Backscattered electron (BSE) image of sample OV-FS-4 (melt abundance is 20.4 ± 0.5 vol% of Fe-S melt). The width of the image is ca. 1.9 mm. Iron sulphide melt: white, olivine: dark grey. Lower panel: BSE image of sample OV-FS-6 (melt abundance is 17.2 ± 1.5 vol%). In 2D, the Fe-S melt appears to form pools with an irregular shape, apparently not forming a continuous network, although conductivity data indicates that the Fe-S melt is interconnected.

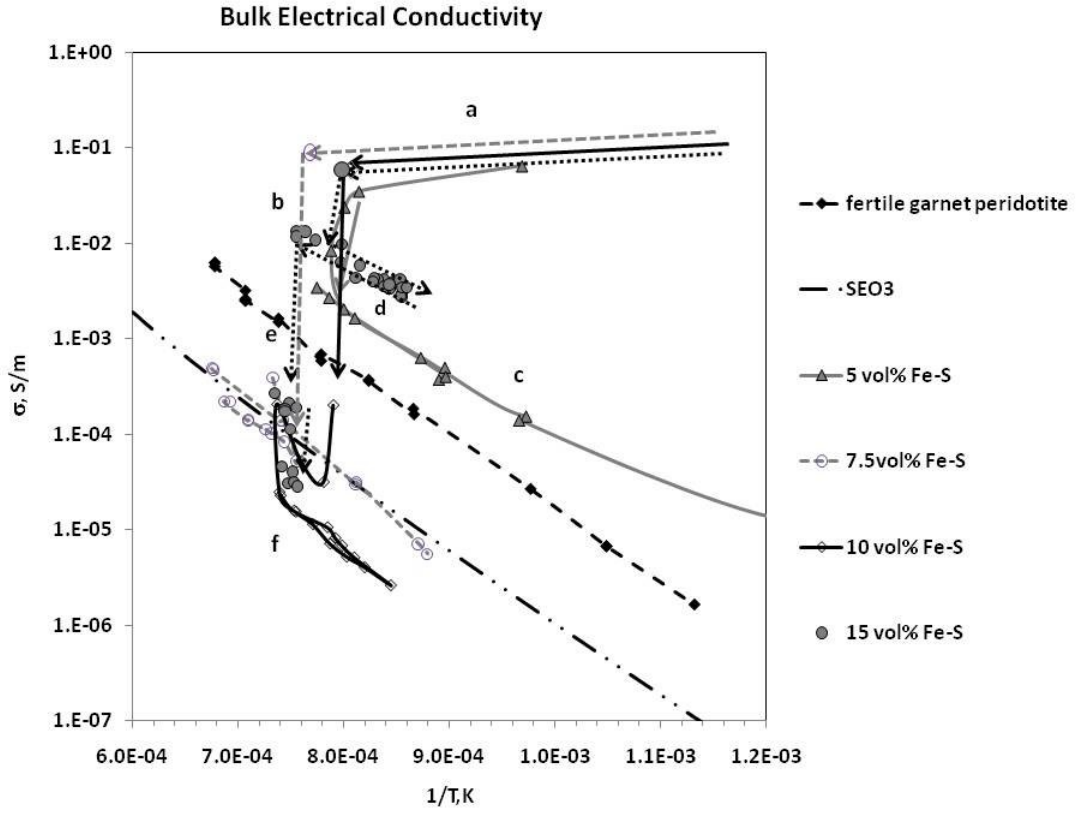

Fig. 4. Summary of electrical conductivity experiments on fertile garnet peridotite samples with various Fe-S content, (*a*) Slow heating up to ca. 980°C. The electrical conductivity is high and corresponds to the conductive network of Fe-S films. (*b*) During annealing at ca. 985 °C over 72 h, the electrical conductivity drops from high values $5 \cdot 10^{-2}$ -10^{-1} S/m to 10^{-3} S/m in the case of the sample with 5 vol% of Fe-S and only to 10^{-2} S/m in the case of the sample with 15 vol% of Fe-S. This may be interpreted as a full disruption of interconnected paths of electrical conductivity due to melting and coagulation of a more conductive Fe-S phase when the Fe-S content is small and partial disruption of Fe-S film when Fe-S content is large. (*c*) During cooling the activation energy of the electrical conductivity corresponds to E_a of fertile garnet peridotite [Bagdassarov et al., 2007]. (*d-e*) In the case of 15 vol% of Fe-S the further heating cycle results in a new step of the electrical conductivity decrease to 10^{-5} S/m at ca. 1060°C. This conductivity is even lower than the conductivity of San Carlos olivine at IW-buffer from Constable [2006]. (*f*) The presence of a large amount of Fe-S (7.5, 10 and 15 vol%) possibly changes the redox environment of the sample and influences the bulk electrical conductivity of the fertile peridotite itself.

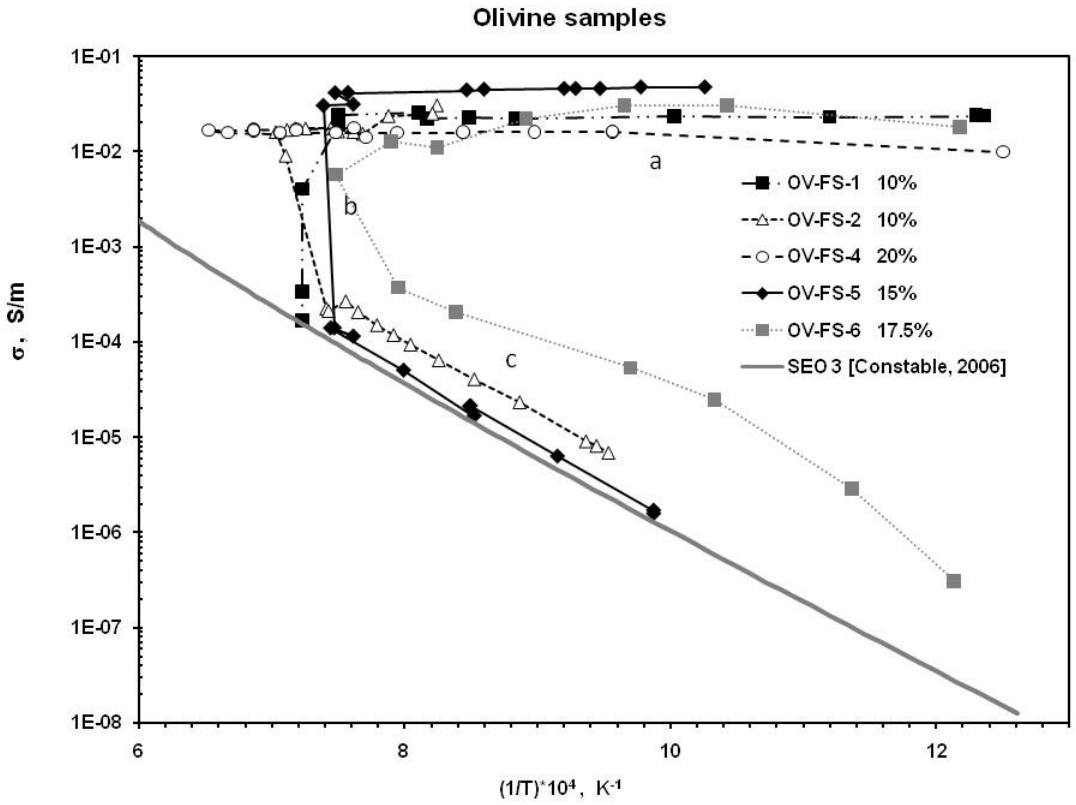

Fig. 5. Variation of the bulk electrical conductivity during annealing experiments for olivine aggregates + Fe-S samples. Heating to the annealing temperature of 900 °C (a) has been done in 20 min. After ca. 70 h of annealing at 900 °C (*b*) the temperature was increased stepwise from 1050 °C to 1110 °C During annealing at ca. 1080°C (b) the electrical conductivity decreased by about 2 orders of magnitude within 2-4 h . In the segment b the temperature has been kept constant. Cooling from *b* to *c* was performed stepwise during ca. 2 h. The electrical conductivity model of San Carlos olivine has been shown for comparison [Constable, 2006].

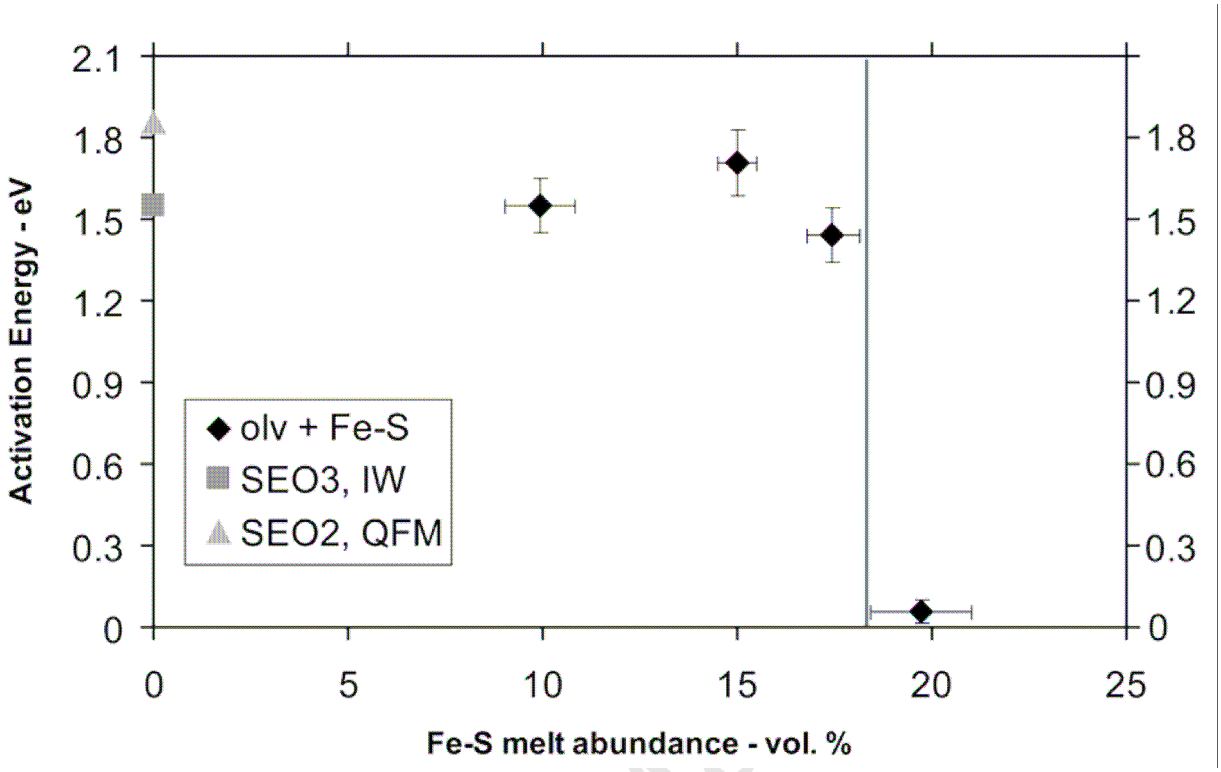

Fig. 6. The activation energy of San Carlos olivine aggregates with Fe-S-melt. The data for Olv + Fe-S are measured for samples OV-FS-2, 4 and 5 (Table 1). The activation energy of pure San Carlos olivine crystals for the oxygen fugacity of IW (SEO3) and of QFM (SEO2) from Constable [2006] is shown for comparison.